Exploiting vibrational resonance in weak-signal detection

Yuhao Ren, Yan Pan, and Fabing Duan*
Institute of Complexity Science, Qingdao University, Qingdao 266071, People's Republic of China

François Chapeau-Blondeau
Laboratoire Angevin de Recherche en Ingénierie des Systèmes (LARIS), Université d'Angers, 62 avenue Notre Dame du Lac, 49000 Angers, France

Derek Abbott
Centre for Biomedical Engineering (CBME) and School of Electrical and Electronic Engineering, University of Adelaide, SA 5005, Australia
(Received 29 December 2016; revised manuscript received 27 April 2017; published 21 August 2017)

In this paper, we investigate the first exploitation of the vibrational resonance (VR) effect to detect weak signals in the presence of strong background noise. By injecting a series of sinusoidal interference signals of the same amplitude but with different frequencies into a generalized correlation detector, we show that the detection probability can be maximized at an appropriate interference amplitude. Based on a dual-Dirac probability density model, we compare the VR method with the stochastic resonance approach via adding dichotomous noise. The compared results indicate that the VR method can achieve a higher detection probability for a wider variety of noise distributions.

DOI: 10.1103/PhysRevE.96.022141

I. INTRODUCTION

Vibrational resonance (VR) proposed by Landa and McClintock [1] is the situation where a high-frequency sinusoidal interference signal of appropriate amplitude can optimally amplify a weak periodic signal in bistable systems. It is also viewed as an interesting alternative to stochastic resonance [2] in which the role of noise is taken over by the vibrational interference [1]. So far, VR has been widely studied in a variety of nonlinear systems such as excitable neurons [3,4], bistable models [5–7], dynamical oscillators [8–10], and circuit systems [11,12]. We inject a series of sinusoidal interfering signals with different frequencies into an array of nonlinear elements, and demonstrate the potential of VR in improving the output-input signal-to-noise ratio (SNR) gain of arrays [13,14]. Moreover, high-frequency vibration or deterministic jitter often naturally arises in real devices [15,16]. Thus, we argue that the VR phenomenon deserves to be further investigated in nonlinear signal processing.

Up to now, there has been little research on the VR effect in statistical signal detection. In this paper, we focus on the potential application of VR in the generalized correlation detector for detecting weak signals buried in a strong noise background. Inspired by the VR mechanism, we inject a series of high-frequency sinusoidal interfering signals of the same tunable amplitude but with different frequencies into nonlinear elements, and then average their outputs to establish a generalized correlation detector. Since this weak signal detection task can be formulated as a statistical hypothesis-test problem, we theoretically analyze the statistical characteristics of this constructed detector, and deduce the normalized asymptotic efficacy with the assumption of a sufficiently large observation length. It is shown that the detection probability of this constructed detector is an increasing function of the number of nonlinear elements and attains its maximum for an infinite number of elements at a given interference amplitude. However, for this limiting case of an infinite number of elements, the detector is not realizable in practice. So we devise an effective realizable detector whose operation is equivalent to that of an infinite number of nonlinear elements, each possessing a given transfer function, and present the theoretical formula for the detection probability. Within this theoretical framework, the VR effect is demonstrated for detecting weak signals buried in a variety of non-Gaussian noise distributions, even when detector parameters vary. It is noted that a dual-Dirac probability density model [15,16] provides an approximation of the amplitude distribution of the sinusoidal vibration. This distribution model is very similar to the distribution of dichotomous noise that induces the stochastic resonance phenomenon [17–21]. Therefore, in the considered generalized correlation detector, we compare the maximum detection probability obtained by high-frequency sinusoidal interfering signals with that achieved by dichotomous noise, and find the VR method attains an improved detection probability for a wider variety of noise distributions. In order to support practical signal detection tasks, we numerically show that the detection probability of a detector with the finite number of elements can closely approach the theoretical detection probability of the impractical detector with an infinite number of elements. These results show that VR is effective in enhancing weak signal detection, without resort to an unrealizable infinite array.

II. MODEL

Consider the observation vector $X=(X_1,X_2,\ldots,X_N)$ of real-valued components X_n given by

$$X_n = \theta s_n + Z_n, \quad n = 1,2,\ldots,N, \tag{1}$$

where s_n represent the known values of signal components with an intensity of $\theta \geqslant 0$, and Z_n are additive zero-mean white

*fabing.duan@gmail.com

noise components with a probability density function (PDF) of f_z. The existence of the signal or not is actually a statistical hypothesis-test problem with the null hypothesis H_0 ($\theta = 0$) and the alternative hypothesis H_1 ($\theta > 0$) [22]. Under the hypotheses H_0 and H_1, the joint probability densities of the observation X are expressed as $f_X(X|H_0) = \prod_{n=1}^{N} f_z(X_n)$ and $f_X(X|H_1) = \prod_{n=1}^{N} f_z(X_n - \theta s_n)$, respectively. It is very difficult to choose H_0 or H_1 in the case of weak signals ($\theta \to 0$). Based on the generalized Neyman-Pearson lemma, the locally optimum or locally most powerful detector can be constructed based on the probability density of noise [22]. However, the optimal detector does not exist for many problems of interest, for instance, unknown noise distributions, or the structure of the optimal detector is too complex to be realized [17,22–26]. Thus, a generalized correlation detector given by

$$T_{\mathrm{GC}}(X) = \sum_{n=1}^{N} g(X_n) s_n \underset{H_0}{\overset{H_1}{\gtrless}} \gamma \tag{2}$$

and is often utilized to select H_0 or H_1 on the basis of X [17,22–26]. Here g is a memoryless transfer function and γ is the decision threshold.

For a sufficiently large observation length N and according to the central limit theorem, the test statistic T_{GC} converges to a Gaussian distribution with expectation $\mathrm{E}(T_{\mathrm{GC}}|H_i)$ and variance $\mathrm{var}(T_{\mathrm{GC}}|H_i)$ under the hypothesis H_i ($i = 0,1$) [22]. Assume the expectation of the memoryless transfer function g is zero under PDF f_z, i.e., $\mathrm{E}[g(x)] = \int_{-\infty}^{\infty} g(x) f_z(x)\, dx = 0$ [22]. Then, for a given a false alarm probability P_{FA}, the detection probability P_{D} can be calculated as

$$P_{\mathrm{D}} = Q[Q^{-1}(P_{\mathrm{FA}}) - \theta\sqrt{N P_s}\sqrt{\xi_{\mathrm{GC}}}], \tag{3}$$

with the function $Q(x) = \int_x^{\infty} \exp[-t^2/2]/\sqrt{2\pi}\, dt$ and the inverse function $Q^{-1}(x)$ [22]. Here the signal power $P_s = \sum_{n=1}^{N} s_n^2/N$, and the normalized asymptotic efficacy ξ_{GC} of the detector is defined as [22,27]

$$\begin{aligned}\xi_{\mathrm{GC}} &= \lim_{N\to\infty}\lim_{\theta\to 0}\left[\frac{\mathrm{E}(T_{\mathrm{GC}}|H_1) - \mathrm{E}(T_{\mathrm{GC}}|H_0)}{\theta\sqrt{N P_s \mathrm{var}(T_{\mathrm{GC}}|H_0)}}\right]^2 \\ &= \lim_{N\to\infty} \frac{\left[\frac{d\mathrm{E}(T_{\mathrm{GC}}|H_1)}{d\theta}\Big|_{\theta=0}\right]^2}{N P_s \mathrm{var}(T_{\mathrm{GC}}|H_0)},\end{aligned} \tag{4}$$

where $\lim_{\theta\to 0}\{\mathrm{E}[T_{\mathrm{GC}}(X)|H_1] - \mathrm{E}[T_{\mathrm{GC}}(X)|H_0]\}/\theta$ tends to the derivative $d\mathrm{E}(T_{\mathrm{GC}}|H_1)/d\theta$ [22].

Inspired by the mechanism of VR, we inject high-frequency sinusoidal interfering signals

$$\eta_{mn} = A_\eta \sin(2\pi f_m n/f_{sa}), \quad m = 1,2,\ldots,M, \tag{5}$$

with the same amplitude A_η but different frequencies f_m into a parallel array of nonlinear elements with the number M, as shown in Fig. 1. Here, we mainly consider the low-pass known signal with a cutoff frequency f_s and the sampling frequency f_{sa}, thus the condition $f_{sa}/2 > f_m \gg f_s$ needs to be satisfied [1,14]. In the discrete-time implementation, the injected frequencies f_m and the sampling frequency f_{sa} are such that $1/f_m$ is always an integer multiple of $1/f_{sa}$. Then, the input of the mth transfer function g is updated as $\widehat{X}_{mn} = X_n + \eta_{mn}$, as shown in Fig. 1. At each time n, we average outputs

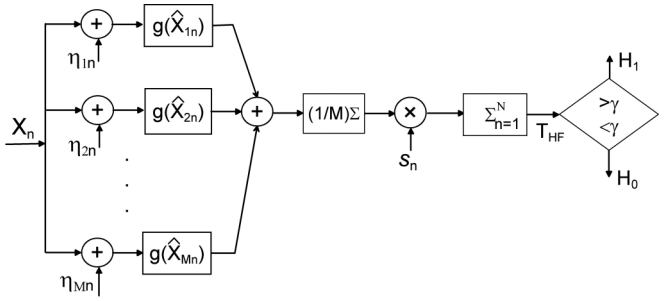

FIG. 1. Generalized correlation detector with M high-frequency sinusoidal interfering signals.

$g(\widehat{X}_{mn})$ and reestablish a generalized correlation detector as

$$T_{\mathrm{HF}}(\widehat{X}) = \sum_{n=1}^{N}\left(\frac{1}{M}\sum_{m=1}^{M} g(\widehat{X}_{mn})\right) s_n \underset{H_0}{\overset{H_1}{\gtrless}} \gamma. \tag{6}$$

Similarly, when the observation length N is sufficiently large, the statistic T_{HF} also converges to a Gaussian distribution, in accordance with the central limit theorem. Then, under the hypothesis H_0, the expectation can be computed as

$$\begin{aligned}\mathrm{E}(T_{\mathrm{HF}}|H_0) &= \frac{1}{M}\sum_{n=1}^{N}\sum_{m=1}^{M}\mathrm{E}[g(\widehat{X}_{mn})]s_n \\ &= \sum_{n=1}^{N}\mathrm{E}[g(\widehat{X}_{mn})]s_n \quad (\forall m \in M) \\ &= 0,\end{aligned} \tag{7}$$

and the variance is given by

$$\begin{aligned}\mathrm{var}(T_{\mathrm{HF}}|H_0) &= \sum_{n=1}^{N}\left[\mathrm{E}\left(T_{\mathrm{HF}}^2|H_0\right) - \mathrm{E}^2(T_{\mathrm{HF}}|H_0)\right] \\ &\approx \frac{1}{M^2}\sum_{n=1}^{N}\left\{\sum_{m=1}^{M}\mathrm{E}[g^2(\widehat{X}_{mn})] + \sum_{\ell=1}^{M}\sum_{k=1}^{M}\right. \\ &\quad \left.\times\,\mathrm{E}[\,g(\widehat{X}_{\ell n})g(\widehat{X}_{kn})]\right\}s_n^2, \quad (\forall \ell \neq k).\end{aligned} \tag{8}$$

Under the hypothesis H_1, the expectation can be evaluated as

$$\mathrm{E}(T_{\mathrm{HF}}|H_1) = \frac{1}{M}\sum_{n=1}^{N}\sum_{m=1}^{M}\mathrm{E}[g(\widehat{X}_{mn})]s_n, \tag{9}$$

and the variance $\mathrm{var}(T_{\mathrm{HF}}|H_1) \approx \mathrm{var}(T_{\mathrm{HF}}|H_0)$ for a very weak signal intensity ($\theta \to 0$). Since the derivative of the expectation of Eq. (9) with respect to θ has no explicit solution, then the normalized asymptotic efficacy in Eq. (4) of the detector in Eq. (6) can not be evaluated. In this case, we turn to calculate the output SNR [22] or the deflection coefficient [27] of the detector in Eq. (6) as

$$R_{\mathrm{out}} = \frac{[\mathrm{E}(T_{\mathrm{HF}}|H_1) - \mathrm{E}(T_{\mathrm{HF}}|H_0)]^2}{\mathrm{var}(T_{\mathrm{HF}}|H_0)}. \tag{10}$$

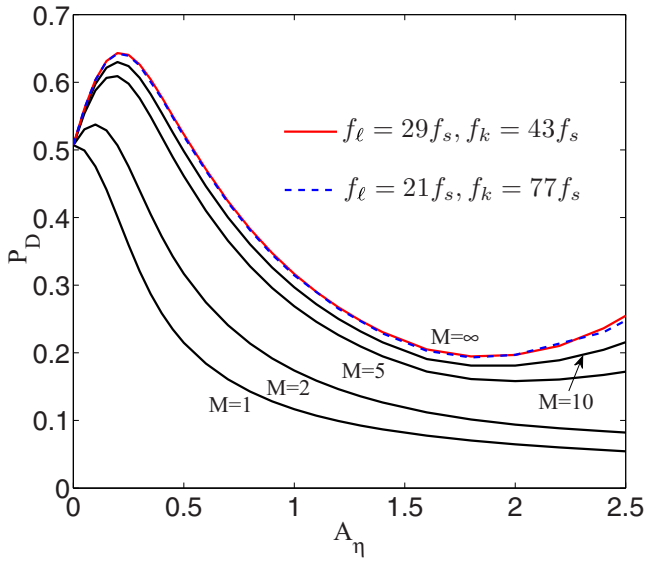

FIG. 2. Theoretical detection probability $P_{\rm D}$ versus the interference amplitude A_η for different numbers $M = 1,2,5,10$, and ∞ of nonlinear elements. Here, the detection probability $P_{\rm D}$ in Eq. (11) can be theoretically computed by the output SNR $R_{\rm out}$ of Eq. (10) for finite numbers of elements $M = 1,2,5$, and 10 (black lines from the bottom up). While, for the infinite number $M = \infty$ of elements, the output SNR $R_{\rm out}$ of Eq. (10) needs to be evaluated by Eqs. (13) and (14). Accordingly, the theoretical detection probabilities $P_{\rm D}$ are plotted versus the interference amplitude A_η for $M = \infty$. The red solid line corresponds to $f_\ell = 29f_s$ and $f_k = 43f_s$, while the blue dashed line represents the theoretical detection probabilities $P_{\rm D}$ obtained as $f_\ell = 21f_s$ and $f_k = 77f_s$. These two lines almost coincide with each other. Here the decay exponent of noise $\alpha = 8$, the threshold $\Theta = 1.6$, the observation length $N = 1000$, the ratio $f_s/f_{sa} = 10^{-3}$, the false alarm probability $P_{\rm FA} = 0.01$, and the input SNR $R_{\rm in} = -25$ dB.

Then, substituting Eqs. (8) and (9) into Eq. (10), we can obtain the detection probability $P_{\rm D}$ in Eq. (3) as [27]

$$\begin{aligned} P_{\rm D} &= Q[Q^{-1}(P_{\rm FA}) - \sqrt{R_{\rm out}}] \\ &= Q[Q^{-1}(P_{\rm FA}) - \theta\sqrt{NP_s}\sqrt{\xi_{\rm HF}}]. \end{aligned} \tag{11}$$

Furthermore, it is demonstrated in Refs. [22,27] that, for the case where the signal strength θ is small, the output SNR $R_{\rm out}$ [22] (or the deflection coefficient [27]) is also related to the normalized asymptotic efficacy $\xi_{\rm HF}$ of the detector in Eq. (6) as

$$\xi_{\rm HF} = \frac{R_{\rm out}}{N\theta^2 P_s}. \tag{12}$$

Based on Eqs. (8) and (9), the detection probability $P_{\rm D}$ of Eq. (11) can be theoretically calculated for a finite number M of nonlinear elements. It is interesting to note that, for a given detector and the signal energy, the normalized asymptotic efficacy is an increasing function of the number M of nonlinear elements [25]. This argument is also verified by the illustrative example of Fig. 2, wherein the detection probability $P_{\rm D}$ attains its maximum for $M = \infty$ elements at a given interference amplitude A_η. Thus, the subsequent discussion will mainly focus on the situation of an infinite number of nonlinear elements. Under this scenario, in order to reduce the computation complexity of Eqs. (8) and (9), we can approximate the expectation of Eq. (9) as

$$\begin{aligned} \mathrm{E}(T_{\rm HF}|H_1)^\infty &= \lim_{M\to\infty}\frac{1}{M}\sum_{n=1}^{N}\sum_{m=1}^{M}\mathrm{E}[g(\widehat{X}_{mn})]s_n \\ &\approx \sum_{n=1}^{N}\mathrm{E}[g(\widehat{X}_{mn})]s_n, \end{aligned} \tag{13}$$

and the variance of Eq. (8) becomes

$$\begin{aligned} \mathrm{var}(T_{\rm HF}|H_0)^\infty &= \lim_{M\to\infty}\sum_{n=1}^{N}\left\{\frac{1}{M^2}\sum_{m=1}^{M}\mathrm{E}[g^2(\widehat{X}_{mn})]\right. \\ &\quad \left.+\frac{1}{M^2}\sum_{\ell=1}^{M}\sum_{k=1}^{M}\mathrm{E}[g(\widehat{X}_{\ell n})g(\widehat{X}_{kn})]\right\}s_n^2 \\ &\approx \sum_{n=1}^{N}\mathrm{E}[g(\widehat{X}_{\ell n})g(\widehat{X}_{kn})]s_n^2, \quad (\ell \neq k), \end{aligned} \tag{14}$$

where the term $\sum_{m=1}^{M}\mathrm{E}[g^2(\widehat{X}_{mn})]$ is $O(M)$, and the term $\sum_{\ell=1}^{M}\sum_{k=1}^{M}\mathrm{E}[g(\widehat{X}_{\ell n})g(\widehat{X}_{kn})]$ is $O(M^2)$. We can regard the sinusoidal interference signal as a variable with the distribution of $f_\eta(x) = 1/(\pi\sqrt{A_\eta^2 - x^2})$, while different frequencies $f_{k,\ell}$ indicate the different samples of this variable. Then there are $M(M-1)$ identical expectations of $\mathrm{E}[g(\widehat{X}_{\ell n})g(\widehat{X}_{kn})] = \mathrm{E}\{\mathrm{E}_\eta^2[g(X_n+\eta_n)]\}$ for any pair of frequencies $f_\ell \neq f_k$. Here the expectation operator $\mathrm{E}_\eta(\cdot) = \int\cdot f_\eta(u)\,du$. Thus, the variance of Eq. (14) can be theoretically evaluated for the infinite number of nonlinear elements.

Moreover, from Eqs. (13) and (14), we find that the indices m, ℓ, and k are generic indices that are arbitrary, but different ($\ell \neq k$). Then, we can adopt two nonlinear parallel elements subjected to the sinusoidal interfering signals $\eta_{\ell n}$ and η_{kn} with frequencies $f_\ell \neq f_k$, respectively. Based on the outputs of $g(\widehat{X}_{\ell n})$ and $g(\widehat{X}_{kn})$, the expectation of Eq. (13) and the variance of Eq. (14) can be obtained. Substituting Eq. (13) and Eq. (14) into Eq. (10), we can theoretically calculate the corresponding detection probability $P_{\rm D}$ of Eq. (11) for the detector in Eq. (6) with an infinite number $M = \infty$ of nonlinear elements. In Sec. III, it will be shown that this calculation method is achievable.

III. RESULTS

The theoretical analyses of Sec. II are applicable to an arbitrary memoryless transfer function that composes the generalized correlation detector of Eq. (6). In this section, for illustration, we consider a three-level transfer function

$$g(x) = \begin{cases} -1, & x \leqslant -\Theta \\ 0, & -\Theta < x \leqslant \Theta \\ 1, & x > \Theta \end{cases}, \tag{15}$$

with the threshold $\Theta \geqslant 0$. Here it is noted that the transfer function g in Eq. (15) is easily implementable in practice and tractable analytically, while offering significant effect for signal detection through VR. Furthermore, the weak signal $\theta s_n = \theta\sin(2\pi f_s n/f_{sa})$ is corrupted by zero-mean generalized

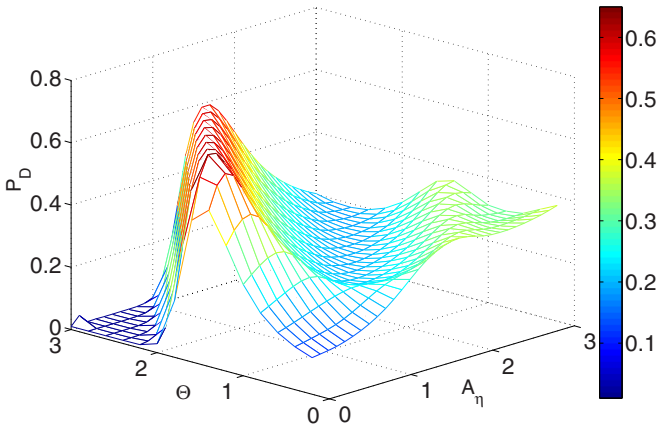

FIG. 3. Detection probability $P_{\rm D}$ versus interference amplitude A_η and threshold Θ. Here the number $M=\infty$ of elements, and the interference frequencies $f_\ell = 29\,f_s$ and $f_k = 43\,f_s$. The other parameters are the same as in Fig. 2.

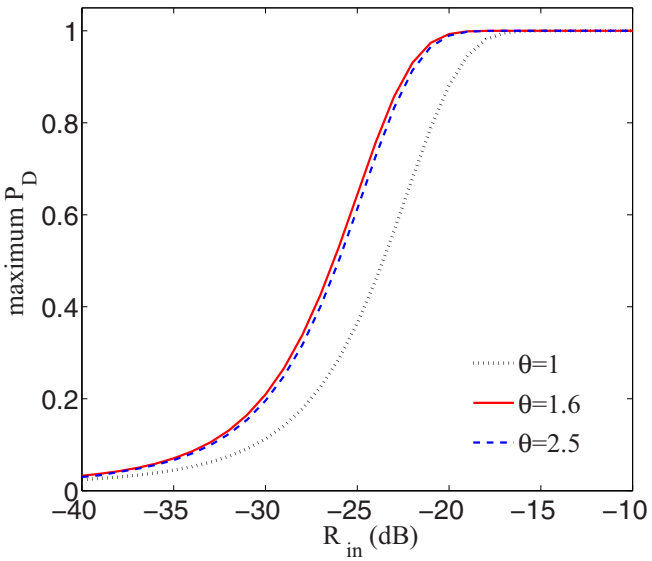

FIG. 4. Maximum of detection probability $P_{\rm D}$ as a function of $R_{\rm in}$ for three threshold values of $\Theta = 1$ (black dotted line), 1.6 (red solid line), and 2.5 (blue dashed line) via optimizing the interference amplitude A_η. The other parameters are the same as in Fig. 3.

Gaussian noise Z_n with its PDF [22,27]

$$f_z(z) = \frac{c_1}{\sigma_z}\exp\left(-c_2\left|\frac{z}{\sigma_z}\right|^{\alpha}\right), \tag{16}$$

where $c_1{=}\frac{\alpha}{2}\Gamma^{\frac{1}{2}}(\frac{3}{\alpha})/\Gamma^{\frac{3}{2}}(\frac{1}{\alpha})$, $c_2{=}[\Gamma(\frac{3}{\alpha})/\Gamma(\frac{1}{\alpha})]^{\frac{\alpha}{2}}$ for a rate of decay exponent $\alpha > 0$, and the variance σ_z^2 is also called noise power P_z. Then, the input SNR is defined as $R_{\rm in} = P_s/P_z = \theta^2/(2\sigma_z^2)$ [22,27]. It is noted that the known input signal is not restricted to the sinusoidal waveform, and other band-limited signals with the same signal power P_s also present the similar enhancement of the detection probability.

For a given input SNR $R_{\rm in} = -25$ dB, the detection probability $P_{\rm D}$ is plotted in Fig. 2 versus the interference amplitude A_η for different numbers $M = 1,2,5,10,\infty$ of elements (black lines from the bottom up). It is seen in Fig. 2 that, as the interference amplitude A_η increases, the detection probability $P_{\rm D}$ exhibits the VR effect, i.e., the enhancement of $P_{\rm D}$ via optimizing the interference amplitude A_η. It is also noted that the detection probability P_D is a monotonic increasing function of the number M of nonlinear elements at a given interference amplitude A_η. For an infinite number $M=\infty$ of elements, we select different frequencies of f_ℓ and f_k to calculate the theoretical detection probability $P_{\rm D}$ of Eq. (11), as shown in Fig. 2. The red solid line represents the detection probability $P_{\rm D}$ for the interfering frequencies of $f_\ell = 29\,f_s$ and $f_k = 43\,f_s$, and the blue dashed line corresponds to the detection probability $P_{\rm D}$ when interference frequencies are $f_\ell = 21\,f_s$ and $f_k = 77\,f_s$ in Eq. (14). These choices of two distinct frequencies are mainly illustrative, and in principle for an infinite number $M=\infty$ of elements, any two distinct frequencies will yield almost the same result.

Next, we plot the detection probability $P_{\rm D}$ versus the interference amplitude A_η and the threshold Θ in Fig. 3 for the decay exponent $\alpha = 8$ and the infinite number $M=\infty$ of elements. It is seen in Fig. 3 that, for a given threshold Θ, the detection probability $P_{\rm D}$ increases in pace with the increase of A_η at first, then reaches a maximum value and finally falls down, this is the VR effect. In addition, $P_{\rm D}$ has another local peak as A_η further increases, which is referred to as the multiresonance effect [1,3,5–9,13,14], as shown in Fig. 3. In our previous studies [13,14], this multiresonance effect is also analyzed for different decay exponents and numbers of nonlinear elements. It is shown in Refs. [13,14] that the multiresonance phenomenon is not only related to the comparison between the nonlinearity and the excitations due to the interferences, but is also associated with the noise type ($\alpha > 2$) and certain numbers $M > 1$. This complicated resonant behavior deserves to be further studied, and we here mainly focus on the maximum detection probability elicited by this multiresonance phenomenon.

We also note in Fig. 3 that, for different values of the threshold Θ, the VR effect still survives. For instance, for given threshold values of $\Theta = 1$ (black dotted line), 1.6 (red solid line) and 2.5 (blue dashed line), the maximum $P_{\rm D}$ is plotted in Fig. 4 as a function of the input SNR $R_{\rm in}$ via optimizing the interference amplitude A_η. It is shown in Fig. 4 that, at each point of $R_{\rm in}$, the largest value of the maximum $P_{\rm D}$ is obtained at the optimal value of the $\Theta = 1.6$. Therefore, the existence of the VR phenomenon in Fig. 3 indicates that the positive role of high-frequency interferences does not disappear for the variable detector composed of the transfer function in Eq. (15). The VR benefit to enhance the detection performance thus exists over a broad range of the threshold Θ, but the VR efficacy is at its best for a specific optimal value of Θ.

Furthermore, the generalized noise model of Eq. (16) describes many noise types encountered in real-world systems, ranging from Gaussian noise ($\alpha = 2$), Laplacian noise ($\alpha = 1$), to uniform noise ($\alpha = \infty$) [22]. Based on the VR method indicated in Fig. 3, we plot the maximum $P_{\rm D}$ (blue asterisks) as a function of the decay exponent α for the given $R_{\rm in} = -25$ dB and $\Theta = 1.6$ in Fig. 5. It is seen in Fig. 5 that, in this considered situation, Gaussian noise is the worst type of background noise for detecting weak signals. We attribute this characteristic to the Fisher information

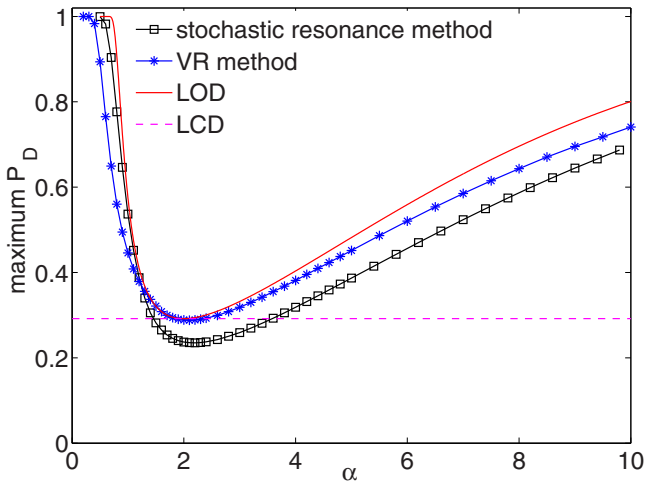

FIG. 5. Theoretical maximum detection probability $P_{\rm D}$ versus the decay exponent α for a given input SNR $R_{\rm in} = -25$ dB and the threshold $\Theta = 1.6$. Here the blue asterisks represent the maximum $P_{\rm D}$ achieved by the VR method, while the black squares represent the maximum $P_{\rm D}$ via the stochastic resonance method. The detection probabilities of the LOD (red solid line) and the LCD (magenta dashed line) are also plotted as a function of the decay exponent α, respectively. The other parameters are the same as in Fig. 3.

$I(f_z) = \alpha^2\Gamma(3\alpha^{-1})\Gamma(2-\alpha^{-1})/[\sigma_z^2\Gamma^2(\alpha^{-1})]$ of the noise distribution [13,14,22], and the Gaussian noise has the minimal Fisher information $I(f_z) = 1/\sigma_z^2$ ($\alpha = 2$) [22]. Here it is noted that the obtained maximum $P_{\rm D}$ (blue asterisks) are the upper bound that this generalized detector of Eq. (6) can achieve, but not the optimal detectability (red solid line) of the locally optimum detector (LOD) in the generalized Neyman-Pearson sense [22,27], as illustrated in Fig. 5. It is known that the normalized asymptotic efficacy in Eq. (4) reaches its maximum of the Fisher information $I(f_z)$, which is achieved by the LOD with the nonlinearity $g(X) = -f_z'(X)/f_z(X)$ in Eq. (2) [22]. The corresponding detection probability $P_{\rm D} = Q[Q^{-1}(P_{\rm FA}) - \theta\sqrt{NP_s}\sqrt{I(f_z)}]$ (red solid line) of the LOD is also illustrated in Fig. 5. It is noted that, due to the benefits of high-frequency interferences, the VR method presents the corresponding detection probability $P_{\rm D}$ (blue asterisks) close to that (red solid line) of the LOD. In addition, the linear correlation detector (LCD) with $g(X) = X$ in Eq. (2) is frequently employed in practice [22], since the Gaussian noise model of the data is well justified and the corresponding optimal detector is the LCD. We note that the detection probability of the LCD is $P_{\rm D} = Q[Q^{-1}(P_{\rm FA}) - \sqrt{NR_{\rm in}}]$ (magenta dashed line). For a given input SNR $R_{\rm in}$, the detection probability of the LCD is a constant for any decay exponent $\alpha > 0$, as shown in Fig. 5. It is interesting to note that, compared with the LCD, the VR method always attains a better detection probability.

In addition, it is shown in Refs. [15,16] that, from the histogram of the ideal timing positions of binary transitions between $\pm A$, a dual-Dirac probability density model

$$f_\eta(\eta) = \tfrac{1}{2}[\delta(\eta - A) + \delta(\eta + A)] \tag{17}$$

provides an appropriate way to approximately represent the amplitude distribution of high-frequency sinusoidal interfering signals. This model is immediately similar to the distribution for dichotomous noise, which randomly takes $+A$ or $-A$ with the same probability of 0.5. Therefore, in this considered detector of Eq. (6), we will compare the maximum detection probability obtained by tuning the amplitude of high-frequency sinusoidal interfering signals with that achieved by tuning the dichotomous noise level.

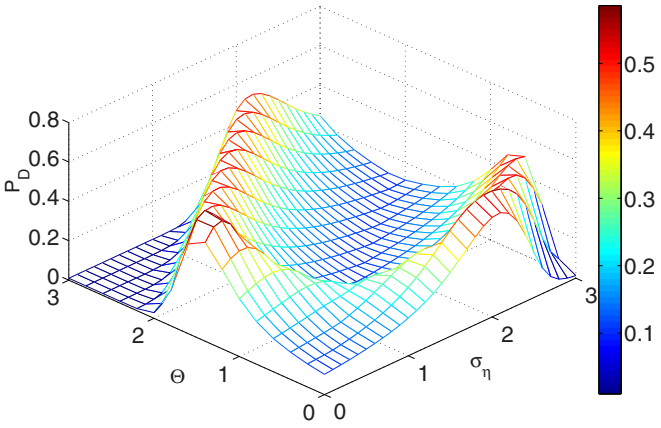

FIG. 6. Detection probability $P_{\rm D}$ as a function of threshold Θ and the dichotomous noise level σ_η. Here the dichotomous noise components, instead of high-frequency sinusoidal interfering signals, is added to the generalized correlation detector of Eq. (6). The other parameters are the same as in Fig. 3.

We inject dichotomous noise into the mth transfer function, and the observation vector is updated as

$$\widetilde{X}_{mn} = \theta s_n + Z_n + \eta_{mn} = \theta s_n + W_{mn}, \tag{18}$$

where η_{mn} represent the dichotomous noise samples in the mth parallel element, and the composite noise components $W_{mn} = Z_n + \eta_{mn}$ have the convolution distribution $f_w(w) = \int f_\eta(u) f_z(w-u)\,du = [f_z(w-\sigma_\eta) + f_z(w+\sigma_\eta)]/2$. Here, the dichotomous noise is with its PDF $f_\eta(\eta) = \frac{1}{2}[\delta(\eta-\sigma_\eta) + \delta(\eta+\sigma_\eta)]$ and variance σ_η^2 [17–21]. Therefore, the hypothesis-test problem becomes a decision on the updated observation data $\widetilde{X}$ to determine whether the weak signal appears or not.

In previous work [25], when the signal amplitude $\theta \to 0$, the normalized asymptotic efficacy in Eq. (4) for a generalized correlation detector with an infinite number $M = \infty$ is given by

$$\begin{aligned}\xi_{\rm GC} &= \lim_{M\to\infty} \frac{{\rm E}_w^2[dg(w)/dw]}{\frac{1}{M}{\rm E}_w[g^2(w)] + \frac{M-1}{M}{\rm E}_z\{{\rm E}_\eta^2[g(\eta+z)]\}} \\ &\approx \frac{{\rm E}_w^2[dg(w)/dw]}{{\rm E}_z\{{\rm E}_\eta^2[g(\eta+z)]\}} \\ &= \frac{4f_w^2[\Theta]}{{\rm E}_z\{{\rm E}_\eta^2[\frac{1}{2}{\rm sign}(\eta+z-\Theta) + \frac{1}{2}{\rm sign}(\eta+z+\Theta)]\}},\end{aligned} \tag{19}$$

where ${\rm E}_v[\cdot] = \int \cdot f_v(v)dv$ for $v = w, z$ and η. Using Eq. (19) and Eq. (3), we plot the detection probability $P_{\rm D}$ in Fig. 6 as a function of threshold Θ and the noise level σ_η. It is seen in Fig. 6 that, at a given $R_{\rm in} = -25$ dB and for the external non-Gaussian noise ($\alpha = 8$), $P_{\rm D}$ also presents the stochastic

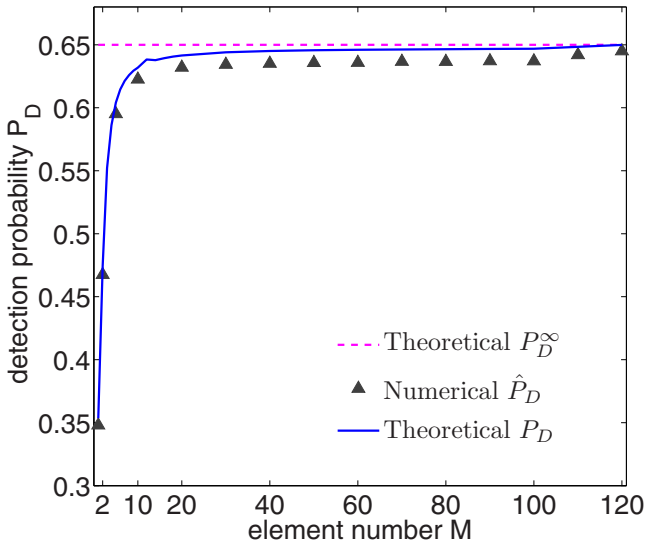

FIG. 7. Numerical and theoretical detection probabilities P_D as a function of the number M of nonlinear elements. For an infinite number $M = \infty$, the theoretical maximum detection probability $P_D = 0.65$ of Eq. (11) (magenta dashed line) is calculated by the output SNR R_{out} of Eq. (10) based on Eqs. (13) and (14). For a finite number $M \geqslant 2$ of elements, the theoretical detection probability P_D of Eq. (11) calculated by Eqs. (8) and (9) is plotted (blue solid line). In numerical experiments, the values of the detection probability (black upper triangles) are achieved by the Monte Carlo simulation method [27]. Based on Eq. (14) and Eq. (2.37) of Ref. [27], the decision threshold $\gamma = Q^{-1}(P_{FA})/\mathrm{var}(T_{HF}|H_0)$ can be obtained for a given false alarm probability $P_{FA} = 0.01$. Then, for the observation size $N = 1000$ and generating N independent random variables Z_n, we compare the statistic T_{HF} in Eq. (6) with the obtained threshold γ for a number of realizations of 10^5, and estimate the detection probability $\hat{P}_D$ as the ratio of the number of $T_{HF} > \gamma$ over the 10^5 realizations. From Eq. (2.38) of Ref. [27], the number of realizations needs to be larger than $[Q^{-1}(\beta/2)]^2(1 - P_D)/\epsilon^2 P_D$. Here the number of realizations 10^5 is large enough for evaluating the detection probability P_D with a relative absolute error $\epsilon = 0.01$ and the confidence level $100(1 - \beta)\%$ ($\beta = 0.05$). Here, the threshold value of the nonlinearity is $\Theta = 1.6$, the input SNR is $R_{in} = -25$ dB, the interference amplitude $A_\eta = 0.2$, and the other parameters are the same as in Fig. 3.

multiresonance effect as the noise level σ_η increases. This kind of multipeak effect has been also observed by tuning the noise (not dichotomous noise) level in the context of stochastic multiresonance [28–30].

The global similarity of Fig. 3 and Fig. 6 indicates the comparable possibility of enhancing the detection of a generalized correlation detector, by injecting the high-frequency interference via VR or by adding noise via stochastic resonance. Here we further observe an interesting feature of the multiresonance effect by comparing the nonlinearity with the amplitude A_η of the high-frequency interference or the noise level σ_η. From Fig. 3 and Fig. 6, it is clearly seen that the location of the main resonance maximum of P_D has linear relationship with a certain offset of the threshold Θ. This result indicates that the superposition of the intrinsic noise Z_n and the external vibration or dichotomous noise η_n forms an effective excitation whose amplitude interacts with the threshold Θ. Thus, even in absence of the external vibration, the intrinsic noise, by tuning its own level, can induce the stochastic resonance effect that defines the offset peak location in the threshold Θ. We also observe that the aforementioned linear interrelationship between the location of the second resonance maximum of P_D and the offset of the threshold Θ.

From Fig. 6, the maximum $P_D = 0.586$ at the threshold $\Theta = 1.6$ and the noise level $\sigma_\eta = 0.2$. While, from the result of Fig. 3 via the VR method, the maximum $P_D = 0.65$ is achieved at the threshold $\Theta = 1.6$ and the high-frequency interference amplitude $A_\eta = 0.2$. For a variety of the decay exponent $\alpha > 0$ of noise, we also depict the corresponding maximum detection probabilities P_D (black squares) of the stochastic resonance method in Fig. 5. It is seen in Fig. 5 that, as the decay exponent $\alpha > 1.2$, the VR method (blue asterisks) is more efficient than the approach of adding dichotomous noise for improving the detection probability.

IV. DISCUSSION

In this paper, we theoretically demonstrate that the VR method can be exploited to improve the detection probability of a weak signal. A series of sinusoidal interfering signals with the same amplitude but different high frequencies is injected into an array of parallel elements that compose the generalized correlation detector. Under such scenarios, the normalized asymptotic efficacy of the detector is theoretically deduced. Specifically, the detector with an infinite number of nonlinear elements is mathematically significant, because the detection probability is an increasing function of the number of nonlinear elements. It is demonstrated that we can simply adopt two arbitrary elements subjected to different high-frequency sinusoidal interfering signals, and theoretically calculate the statistical characteristics of such a detector under both hypotheses. Then, for a given false alarm probability, the normalized asymptotic efficacy and the detection probability can be theoretically calculated. This calculation method is theoretically proved to be effective and realizable, as shown in Figs. 2–5. However, an infinite number of elements is not realizable in practice; yet the statistic T_{HF} in Eq. (6) represents a theoretical asymptotic performance that can be closely approached in practice, with an accessible finite number of elements. In Fig. 7, for a given input SNR $R_{in} = -25$ dB and the interference amplitude $A_\eta = 0.2$, we plot both the numerical and theoretical detection probabilities P_D for different numbers $2 \leqslant M \leqslant 120$ of nonlinear elements. It is seen in Fig. 7 that the numerical results (black upper triangles) agree well with the corresponding theoretical values (blue solid line) of P_D, and the origin of the deviation between numerical and theoretical results is due to some of the approximations made in the derivations of Eq. (8), Eq. (9), and the assumption of the variance $\mathrm{var}(T_{HF}|H_1) \approx \mathrm{var}(T_{HF}|H_0)$ in Sec. II. A more accurate theoretical model needs to be established to reduce the statistical dispersion between numerical and theoretical results of the detection probability in future studies. When the number M increases to 120, the corresponding detection probability $P_D = 0.645$, while the theoretical detection probability of $P_D^\infty = 0.65$ for an infinite number $M = \infty$ (magenta dashed line). Importantly, even for the number $M = 10$, the numerical

detection probability P_D already approaches 0.63. Therefore, in realistic signal detection tasks, we only need average outputs of a finite number of parallel elements and establish the detector of Eq. (6) to determine whether a weak signal exists or not. Of course, the detection probability P_D for a finite number of parallel elements will closely approach but be slightly below P_D^∞ for an infinite number of elements.

The amplitude distribution of high-frequency sinusoidal interfering signals can be approximately described as a dual-Dirac probability density model. This model is similar to the distribution for dichotomous noise. Therefore, in the considered detector, we compare the maximum detection probability obtained by tuning the high-frequency sinusoidal interfering signals with that achieved by tuning the dichotomous noise level. It is shown in Fig. 5 that the VR method, compared to the stochastic resonance approach via tuning dichotomous noise, does achieve a higher detection probability when the noise decay exponent $\alpha > 1.2$. Thus, these results indicate that VR is a potential method for enhancing the performance in weak signal detection. The effect can be exploited via purposeful injection of high-frequency interference signals in the process. But it can also be exploited in devices where vibrations or jitters are already naturally present.

Finally, there remain some open questions: In an array of nonlinear elements, we randomly chose the interfering frequencies that are much larger than the input signal frequency. However, the mutual interference characteristic of the high-frequency sinusoidal signals is not considered. If these high-frequency sinusoidal signals are selected as a set of quadrature waveforms by the Gram-Schmidt algorithm, can the detection probability be further improved? Moreover, can the phases or the amplitudes of these high-frequency sinusoidal signals be randomly set? For some interfering frequencies, the interference signals might be sampled into a discrete quasiperiodic sequences similar to the stochastic modulation. The resonant effects can be also observed (not shown here). Then, can these kind of resonant effects be viewed as stochastic resonance? It is also interesting to explore the unknown signal detection problem within the framework of VR. In practice, for unknown input SNRs and a variety of noise distributions, we need to tune the vibrational amplitude and the nonlinearity threshold to enhance the detection probability. We argue that an adaptive algorithm of adjusting the vibrational amplitude might be a good solution, in which the amplitudes of sinusoidal vibrations do not have to be the same, and can be adaptively adjusted based on real-time measurements of the input signals to maximize the detection probability of a detector. These questions deserve to be further studied.

ACKNOWLEDGMENTS

This work is supported by the National Natural Science Foundation (NNSF) of China (61573202) and the Science and Technology Development Program of Shandong Province (2014GGX101031). We sincerely thank the anonymous reviewers for their comments.

[1] P. Landa and P. McClintock, Vibrational resonance, J. Phys. A **33**, L433 (1993).
[2] R. Benzi, A. Sutera, and A. Vulpiani, The mechanism of stochastic resonance, J. Phys. A **14**, L453 (1981).
[3] E. Ullner, A. Zaikin, J. García-Ojalvo, R. Bascones, and J. Kurths, Vibrational resonance and vibrational propagation in excitable systems, Phys. Lett. A **312**, 348 (2003).
[4] D. L. Hu, J. H. Yang, and X. B. Liu, Vibrational resonance in the FitzHugh-Nagumo system with time-varying delay feedback, Comput. Biol. Med. **45**, 80 (2014).
[5] V. N. Chizhevsky and G. Giacomelli, Experimental and theoretical study of the noise-induced gain degradation in vibrational resonance, Phys. Rev. E **70**, 062101 (2004).
[6] V. N. Chizhevsky and G. Giacomelli, Improvement of signal-to-noise ratio in a bistable optical system: Comparison between vibrational and stochastic resonance, Phys. Rev. A **71**, 011801(R) (2005).
[7] V. N. Chizhevsky, E. Smeu, and G. Giacomelli, Experimental Evidence of "Vibrational Resonance" in an Optical System, Phys. Rev. Lett. **91**, 220602 (2003).
[8] V. M. Gandhimathi, S. Rajasekar, and J. Kurths, Vibrational and stochastic resonances in two coupled overdamped anharmonic oscillators, Phys. Lett. A **360**, 279 (2006).
[9] C. Jeevarathinam, S. Rajasekar, and M. A. F. Sanjuán, Theory and numerics of vibrational resonance in Duffing oscillators with time-delayed feedback, Phys. Rev. E **83**, 066205 (2011).
[10] T. L. M. Djomo Mbong, M. Siewe Siewe, and C. Tchawoua, The effect of the fractional derivative order on vibrational resonance in a special fractional quintic oscillator, Mech. Res. Comm. **78**, 13 (2016).
[11] M. Bordet, S. Morfu, and P. Marquié, Ghost responses of the FitzHugh–Nagumo system induced by colored noise, Chaos, Solitons Fractals **78**, 205 (2015).
[12] P. R. Venkatesh and A. Venkatesan, Vibrational resonance and implementation of dynamic logic gate in a piecewise-linear Murali-Lakshmanan-Chua circuit, Comm. Nonlinear Sci. Numer. Sim. **39**, 271 (2016).
[13] Y. Ren and F. Duan, Theoretical and experimental implementation of vibrational resonance in an array of hard limiters, Physica A **456**, 319 (2016).
[14] F. Duan, F. Chapeau-Blondeau, and D. Abbott, Double-maximum enhancement of signal-to-noise ratio gain via stochastic resonance and vibrational resonance, Phys. Rev. E **90**, 022134 (2014).
[15] R. Stephens, Jitter analysis: The dual-Dirac model, RJ/DJ, and Q-scale, Agilent Technologies white paper (2004).
[16] R. Stephens, Analyzing jitter at high data rates, IEEE Comm. Mag. **42**, S6 (2004).

[17] H. Chen, P. K. Varshney, S. Kay, and J. H. Michels, Noise enhanced nonparametric detection, IEEE Trans. Inf. Theory **55**, 499 (2009).

[18] F. Chapeau-Blondeau and X. Godivier, Theory of stochastic resonance in signal transmission by static nonlinear systems, Phys. Rev. E **55**, 1478 (1997).

[19] J.-H. Li and Y.-X. Han, Phenomenon of stochastic resonance caused by multiplicative asymmetric dichotomous noise, Phys. Rev. E **74**, 051115 (2006).

[20] F. Guo and Y. Zhou, Stochastic resonance in a stochastic bistable system subject to additive white noise and dichotomous noise, Physica A **388**, 3371 (2009).

[21] M. Gitterman and I. Shapiro, Stochastic resonance in a harmonic oscillator with random mass subject to asymmetric dichotomous noise, J. Stat. Phys. **144**, 139 (2011).

[22] S. Kassam, *Signal Detection in Non-Gaussian Noise* (Springer-Verlag, New York, 1988).

[23] B. Kosko and S. Mitaim, Robust stochastic resonance: Signal detection and adaptation in impulsive noise, Phys. Rev. E **64**, 051110 (2001).

[24] L. Zeng, J. Li, and J. Shi, M-ary signal detection via a bistable system in the presence of Lévy noise, Chaos Solitons Fractals **45**, 378 (2012).

[25] F. Duan, F. Chapeau-Blondeau, and D. Abbott, Weak signal detection: Condition for noise induced enhancement, Digital Signal Proc. **23**, 1585 (2013).

[26] A. Patel and B. Kosko, Noise benefits in quantizer-array correlation detection and watermark decoding, IEEE Trans. Signal Proc. **59**, 488 (2011).

[27] S. Kay, *Fundamentals of Statistical Signal Processing–Detection Theory* (Prentice-Hall, Englewood Cliffs, NJ, 1998).

[28] J. M. G. Vilar and J. M. Rubí, Stochastic Multiresonance, Phys. Rev. Lett. **78**, 2882 (1997).

[29] S. Matyjaśkiewicz, A. Krawiecki, J. A. Hołyst, and L. Schimansky-Geier, Stochastic multiresonance due to interplay between noise and fractals, Phys. Rev. E **68**, 016216 (2003).

[30] R. Mankin, K. Laas, T. Laas, and E. Reiter, Stochastic multiresonance and correlation-time-controlled stability for a harmonic oscillator with fluctuating frequency, Phys. Rev. E **78**, 031120 (2008).